BAR Domains as Sensors of Membrane Curvature: The Amphiphysin BAR Structure

Brian J. Peter,* Helen M. Kent,* Ian G. Mills,† Yvonne Vallis, P. Jonathan G. Butler, Philip R. Evans,‡ Harvey T. McMahon‡

The BAR (Bin/amphiphysin/Rvs) domain is the most conserved feature in amphiphysins from yeast to human and is also found in endophilins and nadrins. We solved the structure of the *Drosophila* amphiphysin BAR domain. It is a crescent-shaped dimer that binds preferentially to highly curved negatively charged membranes. With its N-terminal amphipathic helix and BAR domain (N-BAR), amphiphysin can drive membrane curvature in vitro and in vivo. The structure is similar to that of arfaptin2, which we find also binds and tubulates membranes. From this, we predict that BAR domains are in many protein families, including sorting nexins, centaurins, and oligophrenins. The universal and minimal BAR domain is a dimerization, membrane-binding, and curvature-sensing module.

Amphiphysins are proteins that are enriched in the mammalian brain and that bind clathrin, adaptor protein complex 2 (AP2), dynamin, and synaptojanin and are proposed to function in synaptic vesicle endocytosis (*1*–*6*). In *Drosophila*, the protein is not enriched in synapses but is instead associated with the muscle T-tubule network and areas of membrane remodeling (*7*–*10*). A splice form of mammalian amphiphysin2 has a similar localization and function in muscle cells (*11*). The only conserved feature of all amphiphysins from yeast to *Drosophila* and humans is an N-terminal BAR domain (pfam03114;SMART00721), which binds and tubulates liposomes in vitro (*7*, *12*). A similar domain is also found in the endophilin family, proteins essential for synaptic vesicle recycling in *Drosophila* (*13*, *14*) and also associated with intracellular organelles (*15*). Endophilin binds and curves membranes in vitro (*16*), although its BAR domain has also been reported to have an additional lysophosphatidic acid acyl transferase activity (*17*). We set out to understand the basic mechanism of curvature generation by the BAR domain.

Structure of *Drosophila* amphiphysin BAR. The structure of the N-terminus of *Drosophila* amphiphysin (dAmph, residues 1 to 245) was determined by x-ray crystallography (Fig. 1, A to D; movie S1; table S1) (*18*). It is an elongated banana-shaped dimer. Each monomer is a coiled-coil of three long kinked α helices, forming a six-helix bundle around the dimer interface. The curvature of the dimer is partly due to the way the monomers intersect and partly due to the kinks in helices 2 and 3. The interface between the monomers is largely hydrophobic (see dimer contacts, black oval symbols in Fig. 1E). By analytical ultracentrifugation, the K_d of the dimer was 6 μM (fig. S1), which may mean that the protein is found as a monomer:dimer equilibrium in vivo. The N-terminus is disordered before residue 26, and the C-terminus is disordered beyond residue 242. The BAR domain, as defined by the crystal structure, spans residues 35 to 240, and it is this region that is homologous in the diverse protein families that we discuss below. The N-terminal unstructured residues are predicted to form an amphipathic helix, and we refer to the amphipathic helix plus the BAR as an N-BAR. On lipid binding, the helical content of the N-BAR domain of amphiphysin increased, as shown by circular dichroism spectroscopy (fig. S2B), which suggested that the N-terminus folded into an extra helix. This increase in helical content is not seen when residues 1 to 26 are deleted. Endophilin also has an N-BAR domain, as has nadrin (also called RICH; fig. S2A), a neuron-specific guanosine triphosphatase (GTPase)–activating protein involved in regulated exocytosis (*19*, *20*).

The positively charged loop between helices 2 and 3 found at the extreme ends of the dimer is flexible and poorly ordered (residues 158 to 165 in dAmph) and is the location of a splice variant in mammalian amphiphysin2 (residues 173 to 205 in Fig. 1E). The concave surface of the dimer also has several positively charged patches (Fig. 1, B and D), which suggests that this is the surface that interacts with phospholipid membranes. This would fit a curved membrane with a diameter of ~220 Å.

Lipid binding and membrane bending are coupled. *Drosophila* amphiphysin binds and tubulates liposomes in vitro, and in vivo, this N-BAR protein is essential for the formation and stability of the muscle T-tubule network (*7*). To test if this tubulating ability is due to the *Drosophila* amphiphysin BAR domain, we mutated pairs of basic residues to glutamates, Lys^{161} + Lys^{163} on the disordered loop between helices 2 and 3 (mut1) and Lys^{137} + Arg^{140} on the concave face (mut2). Neither of these mutations interfered with the structure, and both double-mutants reduced the binding to liposomes; the quadruple-mutant (mut3) was more effective (Fig. 2A). These mutants also effectively inhibited the tubulation of liposomes as assessed by electron microscopy (Fig. 2B). At higher concentrations, the double-mutants showed some tubulation, whereas the quadruple-mutant did not. The tubulating activity of wild-type N-BAR is concentration-dependent (Fig. 2C). At low concentrations, small buds that look like "panhandles" on liposomes were observed (*21*). At intermediate concentrations, tubules predominated, and at still higher concentrations, the liposomes vesiculated. Thus the N-BAR domain is capable of introducing three-dimensional curvature.

Equivalent double mutations were also made in mammalian amphiphysins 1 and 2 of lysine residues in the loop between helices 2 and 3, which correspond to mut1 in *Drosophila* amphiphysin N-BAR. These double-mutants reduced liposome binding (Fig. 2D), and liposome tubulation was severely inhibited (Fig. 2E).

The amphipathic helix at the N-terminus of the BAR domain is important but not essential for tubulation. Deletion of residues 1 to 26 of *Drosophila* amphiphysin or residues 1 to 27 in mammalian amphiphysin1, or mutation of Phe^{9} to glutamate, reduced liposome binding as expected (*16*), but these proteins still tubulated at high concentrations (Fig. 2, B and E). The folding of this helix could aid tubulation by direct interaction with the membrane and/or by protein-protein interactions between dimers, but we cannot distinguish these mechanisms at present.

The amphiphysin1 N-BAR also tubulated membranes when overexpressed in COS cells (Fig. 2F and fig. S3A). Some of these tubules emanated from the plasma membrane and were accessible to the membrane fluorescent dye FM2-10. Mut1 was also effective in vivo to prevent membrane association and tubulation (Fig. 2F). Overexpression of the N-BAR domain from the leukemia-associated antigen BRAP1/Bin2 (*22*, *23*) also resulted in tubular structures in cells, whereas mutations analogous to mut1 blocked this effect (fig. S3B).

As a functional test of the amphiphysin BAR domain, we tested the ability of amphiphysin2 to

Medical Research Council (MRC) Laboratory of Molecular Biology, Hills Road, Cambridge CB2 2QH, UK.

*These authors contributed equally to this work.
†Present address: Department of Oncology, University of Cambridge, Hutchison/MRC Cancer Research Centre, Hills Road, Cambridge CB2 2XZ, UK.
‡To whom correspondence should be addressed. E-mail: hmm@mrc-lmb.cam.ac.uk (H.T.M.); pre@mrc-lmb.cam.ac.uk (P.R.E.)

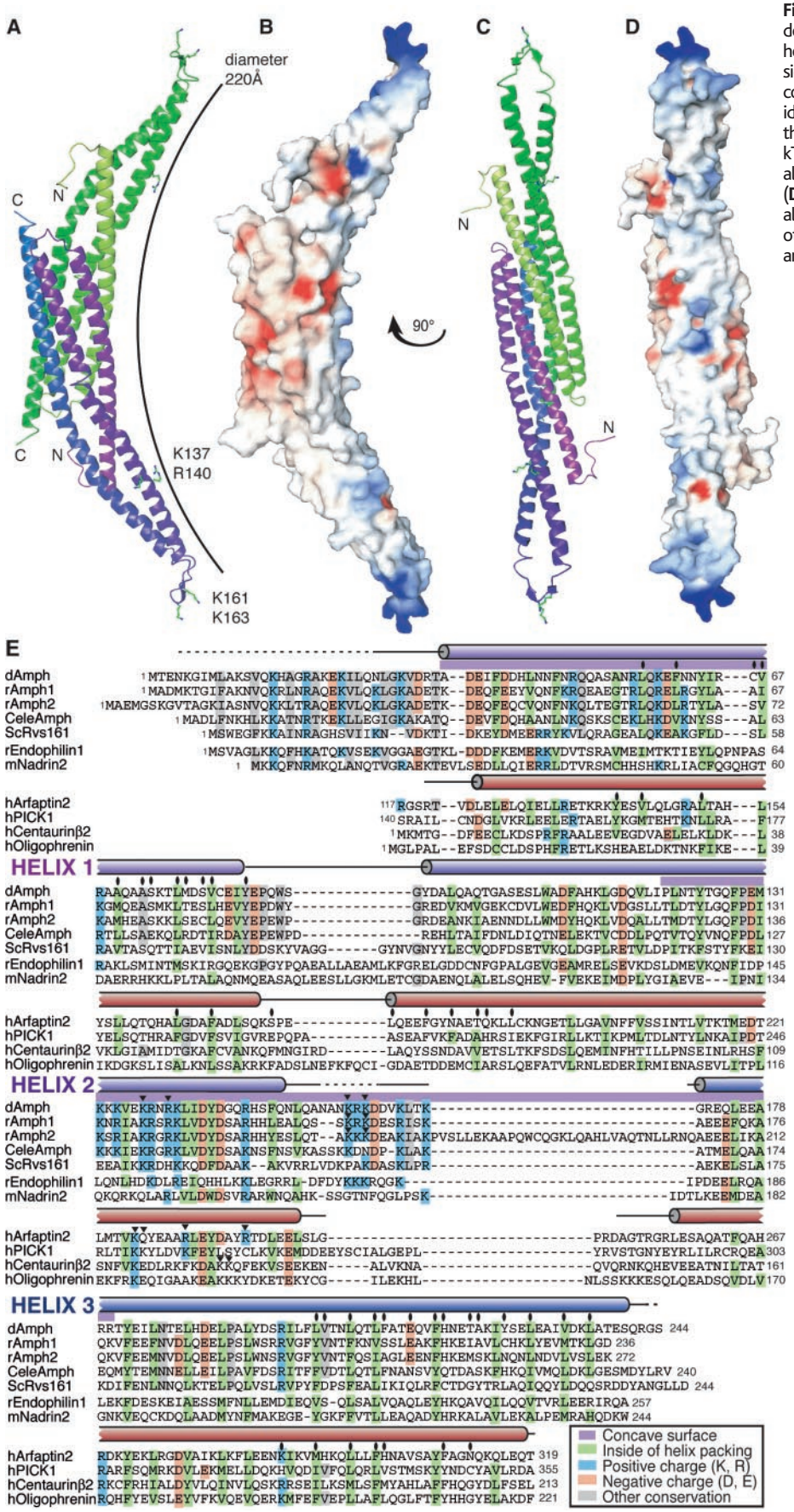

Fig. 1. Structure of the *Drosophila* amphiphysin BAR domain. (**A**) Ribbon representation of the antiparallel homodimer (purple and green monomers). The principal side chains that make up the positive patches on the convex surface are marked. Protein Data Bank (PDB) identification (ID): 1URU. (**B**) Same view as in (A), with the surface colored by electrostatic potential (red, −10 kTe^{-1}, blue, +10 kTe^{-1}). (**C**) Ribbon diagram viewed along the dyad axis (concave face) perpendicular to (A). (**D**) Electrostatic surface viewed as in (C). (**E**) Sequence alignment of the BAR domains in amphiphysins and other proteins (*53*). Black triangles indicate mutations, and ovals indicate dimer contacts in the structures.

recruit clathrin to membranes. Mammalian amphiphysin2 has several clathrin-binding sites (*24*–*26*), and we found that the wild-type, but not mut1, efficiently recruited clathrin to liposomes (fig. S4A). Furthermore, we found that amphiphysin2 was able to polymerize clathrin into invaginated lattices on a lipid monolayer, whereas mut1 amphiphysin2 was only able to form clathrin cages in solution (fig. S4B). Thus, amphiphysin is like AP180 (*27*) in its ability to recruit and polymerize clathrin into uniform patches/caps, and this depends on a functional BAR domain.

Arfaptin2 has a BAR domain. The structure of the amphiphysin BAR is very similar to the C-terminal domain of arfaptin2 (*28*) (Fig. 3A and fig. S5), despite very weak sequence homology (Fig. 1E). Both are banana-shaped helix bundles with positive charge density at the extremities and on the concave surface. Arfaptin (also called POR1) has been shown to bind to the GTP-binding proteins (G proteins) Arf, Arl, and Rac (*28*–*31*), but the similarity to amphiphysin suggested to us that arfaptins may bind to membranes independently of small G proteins. Wild-type full-length arfaptin2 (hereafter, arfaptin) bound more effectively to liver liposomes than to brain liposomes or synthetic liposomes containing phosphatidylinositol-4,5-bisphosphate [PtdIns(4,5)P_2] (Fig. 3B). On nitrocellulose membranes, arfaptin bound the phosphatidyl inositol phosphates PtdIns(4)P and PtdIns(3)P (*32*), and in vivo at low levels of overexpression, the protein had a perinuclear distribution like that of endogenous arfaptin (Fig. 3D) and colocalized with the trans-Golgi marker TGN46 (fig. S6). In vitro, arfaptin tubulated liver liposomes (Fig. 3C), but not brain liposomes, and lipid binding was more effective for the full-length protein than for either the BAR or N-terminal domains alone (Fig. 3B). Mutation of the positive charges on the concave face of the BAR domain (fig. S5) prevented the tubulation in vitro and TGN association in vivo (Fig. 3, C and D, and fig. S6). We predict from the structure of the arfaptin-Rac complex (*28*) that these mutations will have no effect on G-protein binding. This possible crosstalk has not been investigated further, but we note that other BAR proteins discussed below are also predicted to bind to small G proteins. In solution, arfaptin was a dimer with K_d of

15 μM (*33*). We conclude that the C-terminal domain of arfaptin is a BAR domain: a dimerization, membrane-binding, and (at least in vitro) bending module.

BAR domains found in other proteins. We searched the sequence database for the presence of BAR domains in other proteins (for some examples, see Fig. 4), and discovered BARs in many different contexts. Some BAR proteins have additional lipid interactions through adjacent pleckstrin homology (PH) or phox homology (PX) domains. Often BAR domains are combined with GEF (guanine nucleotide exchange factor) and GAP (GTP hydrolysis–activating protein) domains, which regulate the activity of small GTPases. A subgroup of proteins (N-BAR proteins) has an N-terminal amphipathic helix similar to the amphiphysins (see also fig. S2A). Another class of BAR proteins that we have not investigated further are proteins like PICK1 and ICA69 (*34*). For many of these proteins, this prediction of a BAR domain is the first, to our knowledge (Fig. 1E). We now confirm this for arfaptin2, nadrin2, centaurinβ2, and oligophrenin1.

As predicted, the N-BAR of nadrin2 (see fig. S2A) binds very well to both synthetic PtdIns(4,5)P_2 liposomes and brain liposomes, which it tubulates efficiently (Fig. 4, B and C). By velocity centrifugation, the protein is a dimer (*33*).

β Centaurins are proposed to modulate vesicular trafficking and actin rearrangements (*35*–*37*) and have more distantly related BAR domains adjacent to PH domains. Centaurins β1/ACAP1, β2/ACAP2, β3/Papα, β4/ASAP1/Ddef1, and β5 all have N-terminal BAR domains (Fig. 4A). The BAR + PH domain of centaurinβ2 was a dimer [K_d 5 μM, (*33*)], and it bound and tubulated liposomes (Fig. 4, B and C) (*38*). The PH domain bound to liposomes but did not tubulate them, whereas the BAR domain alone showed only weak binding (Fig. 4, B and C). In vivo overexpression of the BAR + PH domain also led to membrane tubulation (Fig. 4D) and affected transferrin trafficking (although not endocytosis from the plasma membrane, fig. S3C), whereas mutation of Lys^{124} and Lys^{125} to glutamates completely prevented the tubulation and trafficking defect.

Oligophrenin1 is an F-actin–binding protein in which mutations are associated with X-linked mental retardation (*39*, *40*). Other members of the oligophrenin family include GRAF and PSGAP (*41*, *42*), which have BARs and a similar domain structure. Like centaurinβ2, the oligophrenin BAR + PH domain tubulated liposomes (Fig. 4C) (*38*).

BAR domains as sensors of curvature. We predicted that the curved BAR domain may bind more tightly to curved than to flat membranes. A protein will curve membranes if the difference in the energy of binding to curved versus flat membranes is greater than the energy required for membrane deformation. If the difference in binding energies is insufficient for deformation, a protein may still prefer preexisting curved membranes, that is, it may sense curvature. We would expect the curved BAR domain to recognize curved membranes, even for examples such as oligophrenin and centaurinβ2, which tubulated inefficiently. We tested this using liposomes of different intrinsic curvatures (Fig. 5A). Oligophrenin and centaurin BAR + PH proteins were sensitive to the vesicle size and, thus, to the extent of curvature (Fig. 5B). This curvature-sensing effect was seen with the centaurin BAR domain alone (despite the weak interaction with liposomes) and was not seen for the PTB domain from Dab2 (*43*), which serves as a control for the available binding surface of the different liposomes. In contrast, proteins that tubulated efficiently, such as the epsin1 ENTH domain (*44*), arfaptin, and the amphiphysin and nadrin N-BARs, all bound independently of liposome curvature [Fig. 5C and (*32*)]. Deletion of the amphipathic helix from amphiphysin (changing the N-BAR to a simple

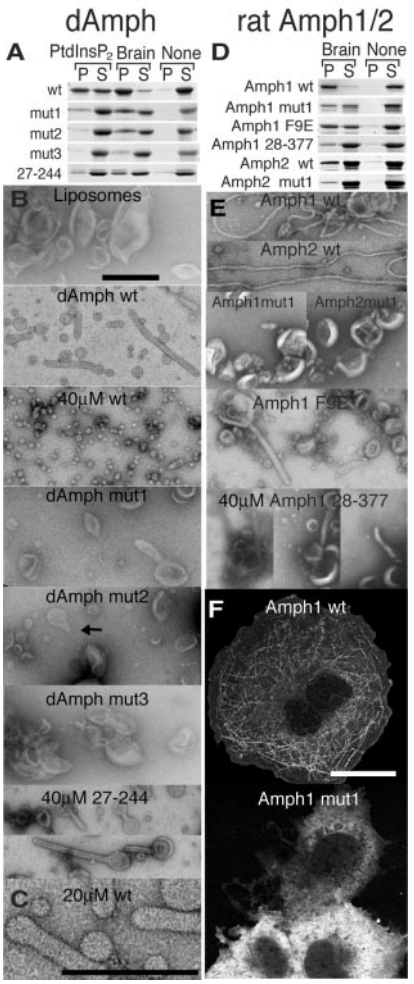

Fig. 2. Membrane binding and tubulation by amphiphysins: (left) *Drosophila* amphiphysin and (right) rat amphiphysins 1 and 2. (**A**) Coomassie-stained gels of sedimentation assays with synthetic liposomes containing 10% PtdIns(4,5)P_2, liposomes made from total brain lipids, or no liposomes. Mut1 has the glutamate substitutions K161E + K163E; mut2 has K137E + R140E; mut3 is mut1 and mut2 combined; 27-244 is the BAR alone. Wt, wild-type; P, pellet; and S, supernatant. (**B**) Electron micrographs of brain liposomes incubated with the indicated proteins at 5 μM concentration unless otherwise indicated. Some liposomes exhibit buds, which may be the beginnings of tubes (arrow). Scale bar of 300 nm applies to all micrographs except (C) and (F). (**C**) Striations are visible at higher magnification [see also (*12*)]. The outer diameter of this negatively stained tubule is 46 ± 2 nm. Scale bar, 300 nm. (**D**) Liposome sedimentation assays with brain lipids as in (A). Mut1 has the glutamate substitutions K159E + K161E in amphiphysin1 and K164E + K166E in amphiphysin2. P, pellet; and S, supernatant. (**E**) Electron micrographs of brain liposomes incubated with wild-type (wt) and mutant rat amphiphysin1 and 2. (**F**) COS-7 cells overexpressing rat amphiphysin1 wild-type and mut1. Scale bar, 20 μm.

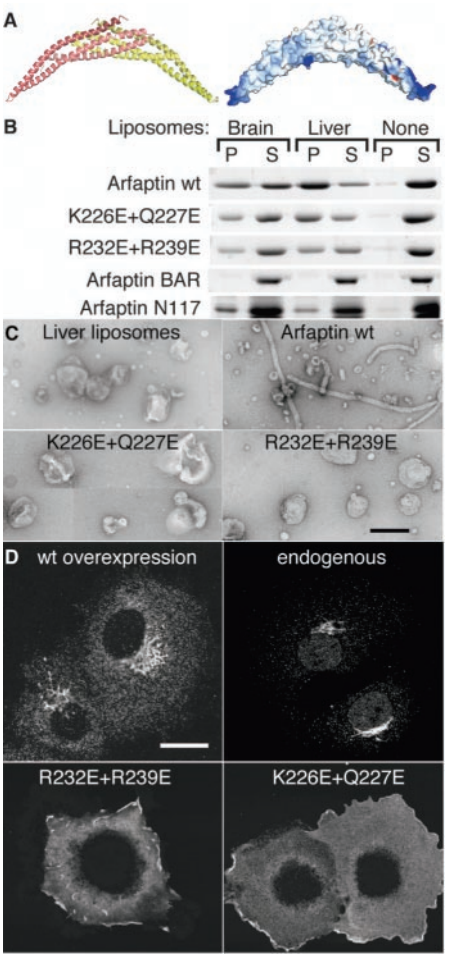

Fig. 3. Arfaptin contains a BAR domain. (**A**) Ribbon diagram (monomers in pink and yellow, left) and electrostatic surface (right) of the arfaptin2 dimer (PDB ID: 1I4D), viewed as in Fig. 1 (A and B). Higher-resolution images and an overlay with the *Drosophila* amphiphysin BAR can be seen in fig. S5. (**B**) Sedimentation assays with wild-type (wt) and mutant full-length arfaptins, the arfaptin BAR alone, and the arfaptin N-terminus (N117) using liposomes made from total brain lipids or total liver lipids. P, pellet; S, supernatant. (**C**) Electron micrographs of liver liposomes incubated with full-length arfaptin and the indicated mutants at 5 μM. Scale bar, 300 nm. (**D**) COS-7 cells expressing wild-type (wt) arfaptin and mutants. Scale bar, 20 μm.

BAR) reduced the overall binding, but it was now sensitive to curvature (*45*). Thus, the most general function of the BAR alone is to sense curvature.

In vesicles coated with coat protein complex I (COPI) or clathrin/AP1, Arf-GTP is important in coat recruitment and invagination. Our observations now provide a possible explanation for how GTP hydrolysis of Arfs, which in COPI-coated vesicles is known as the trigger for uncoating (*46*), can be sensitive to the extent of invagination of the coated vesicle. Many Arf-GAP proteins (only some of which are mentioned in Fig. 4) have BAR domains, and therefore, it is likely that the uncoating event triggered by GTP hydrolysis will only occur when the correct membrane curvature is sensed by the BAR. It is interesting to note that the structure of the COPII prebudding complex (*47*), composed of the Sec23/24 GAP and the Sar1 GTPase, is also concave on the membrane-interacting face.

None of the BAR domains we tested have strong lipid specificities (*48*), but a neighboring PH or PX domain could confer this. The PH or PX domains could target a protein to a specific membrane compartment, while the BAR simultaneously detects membrane curvature; thus, together they may act as a coincidence detector. Our experiments with centaurinβ2 show that both the PH domain and a wild-type BAR domain were required for binding to curved membranes in cells. The BAR + PH domain was localized to membrane tubules (Fig. 4D), but mutations in the lipid-binding surface of the BAR domain or the PH domain or deletion of either domain resulted in a cytoplasmic distribution. The ability to coselect the lipid composition and curvature in proteins like the centaurins, sorting nexins, and oligophrenins allows the cell to localize binding partners precisely to membrane subdomains. It would also allow GAP activities of centaurins and oligophrenins to be restricted to specific regions on organelles. It has been previously noted that the in vivo GAP activity of oligophrenin is regulated by the N-terminus, which is the BAR domain (*39*).

The BAR domain is a dimerization, membrane-binding, and curvature-sensing module, which is found across genomes and in many different protein contexts. Although dimerizing domains and lipid-binding domains are common in proteins, the ability of the BAR to sense curvature suggests another mechanism for the spatial and temporal compartmentalization of proteins to specific membrane domains.

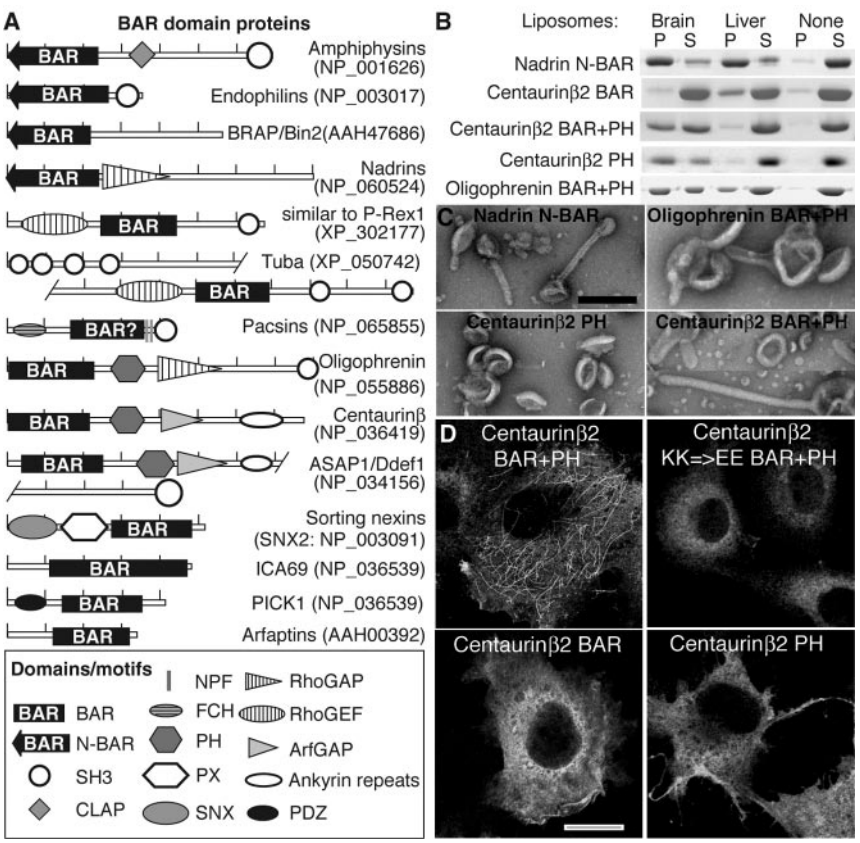

Fig. 4. BAR domains in other proteins. (**A**) BAR domain proteins organized according to the degree of homology to amphiphysin (top) and arfaptin (bottom). We tested the presence of BAR domains in some of these proteins in this paper. Some proteins have very strong homology [Tuba (*54*) and sorting nexins]; others have weaker homology (pacsins and ICA69 with its extended α-helical domain), and there are many others that can be found using BLAST. Protein accession numbers for human (or mouse, for ASAP1) examples in each family are in parentheses. Ticks are every 100 amino acids. Domain descriptions: N-BAR, BAR with an N-terminal amphipathic helix; SH3, binds proline-rich sequences; CLAP, binds clathrin/adaptor proteins; NPF, binds Eps15 homology domains; FCH, Fes/CIP4 homology; PH and PX, phosphoinositide-binding domains; SNX, sorting nexin domain; RhoGAP, GTPase-activating region for Rho GTPases; RhoGEF, guanine nucleotide exchange factor for Rho GTPases; ArfGAP, GTPase-activating region for Arf GTPases; and ankyrin and PDZ, protein-protein interaction domains. For further definitions of these conserved domains and alignments, see the NCBI conserved domain database (*55*). (**B**) Coomassie-stained gels of sedimentation assays with brain and liver liposomes. P, pellet; S, supernatant. (**C**) Electron micrographs of brain liposomes incubated with the indicated proteins at the following concentrations: nadrin2 N-BAR, 15 μM; oligophrenin BAR + PH and centaurinβ2 PH, 40 μM; centaurinβ2 BAR + PH, 25 μM. Scale bar, 300 nm. (**D**) COS-7 cells overexpressing wild-type centaurinβ2 BAR + PH, BAR alone, PH alone, and K124E + K125E BAR + PH domains. Scale bar, 20 μm.

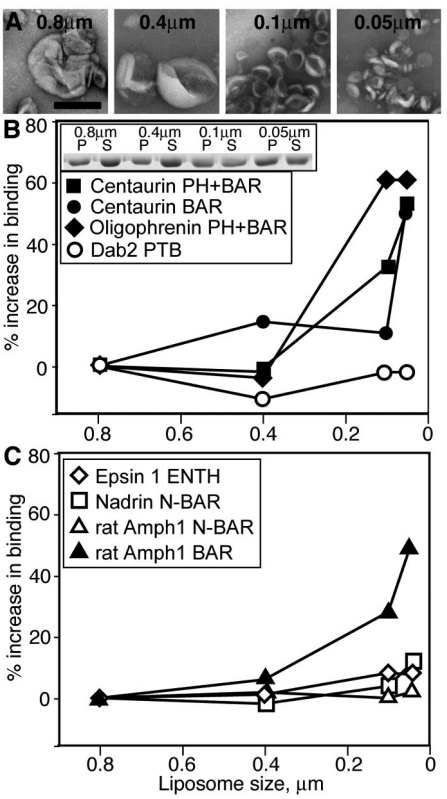

Fig. 5. Curvature sensing by BAR domains. Brain liposomes of different intrinsic membrane curvatures were prepared and sequentially extruded through polycarbonate membranes with pores of 0.8, 0.4, 0.1, and 0.05 μm (*56*). (**A**) Electron micrographs of the liposomes after extrusion. The large vesicle preparations also contained many smaller vesicles; the smaller vesicle preparations were more homogeneous. Scale bar, 300 nm. (**B**) Liposome sedimentation assays were normalized by setting the amount of binding to the largest liposomes to 100%. The PtdIns(4,5)P_2-binding protein Dab2 does not effect curvature and serves as a control for the available surface area of the liposomes. Inset: an example gel showing the liposome sedimentation results for oligophrenin BAR + PH. P, pellet; S, supernatant. (**C**) Liposome sedimentation assays as in (B) showing the effect of deleting the N-terminal amphipathic helix in amphiphysin1.

References and Notes

1. C. David, P. S. McPherson, O. Mundigl, P. De Camilli, *Proc. Natl. Acad. Sci. U.S.A.* **93**, 331 (1996).
2. O. Shupliakov *et al.*, *Science* **276**, 259 (1997).
3. P. Wigge, Y. Vallis, H. T. McMahon, *Curr. Biol.* **7**, 554 (1997).
4. P. Wigge *et al.*, *Mol. Biol. Cell* **8**, 2003 (1997).
5. A. R. Ramjaun, K. D. Micheva, I. Bouchelet, P. S. McPherson, *J. Biol. Chem.* **272**, 16700 (1997).
6. G. Di Paolo *et al.*, *Neuron* **33**, 789 (2002).
7. A. Razzaq *et al.*, *Genes Dev.* **15**, 2967 (2001).
8. A. C. Zelhof *et al.*, *Development* **128**, 5005 (2001).
9. P. A. Leventis *et al.*, *Traffic* **2**, 839 (2001).
10. B. Zhang, A. C. Zelhof, *Traffic* **3**, 452 (2002).
11. E. Lee *et al.*, *Science* **297**, 1193 (2002).
12. K. Takei, V. I. Slepnev, V. Haucke, P. De Camilli, *Nature Cell Biol.* **1**, 33 (1999).
13. A. Guichet *et al.*, *EMBO J.* **21**, 1661 (2002).
14. P. Verstreken *et al.*, *Cell* **109**, 101 (2002).
15. J. Modregger, A. A. Schmidt, B. Ritter, W. B. Huttner, M. Plomann, *J. Biol. Chem.* **278**, 4160 (2003).
16. K. Farsad *et al.*, *J. Cell Biol.* **155**, 193 (2001).
17. A. Schmidt *et al.*, *Nature* **401**, 133 (1999).
18. Materials and methods are available as supporting material on *Science* Online.
19. A. Harada *et al.*, *J. Biol. Chem.* **275**, 36885 (2000).
20. N. Richnau, P. Aspenstrom, *J. Biol. Chem.* **276**, 35060 (2001).
21. We did not see this pan-handle intermediate in our studies of epsin ENTH tubulation (*27*), which implies that the mechanism of tubulation is different. With epsin, we observed an all-or-none tubulation of individual liposomes, whereas amphiphysin initiated a bud and, with higher concentrations, completed the tubule formation.
22. K. Ge, G. C. Prendergast, *Genomics* **67**, 210 (2000).
23. J. Greiner *et al.*, *Int. J. Cancer* **106**, 224 (2003).
24. H. T. McMahon, P. Wigge, C. Smith, *FEBS Lett.* **413**, 319 (1997).
25. V. I. Slepnev, G. C. Ochoa, M. H. Butler, P. De Camilli, *J. Biol. Chem.* **275**, 17583 (2000).
26. M. T. Drake, L. M. Traub, *J. Biol. Chem.* **276**, 28700 (2001).
27. M. G. Ford *et al.*, *Science* **291**, 1051 (2001).
28. C. Tarricone *et al.*, *Nature* **411**, 215 (2001).
29. O. H. Shin, J. H. Exton, *Biochem. Biophys. Res. Commun.* **285**, 1267 (2001).
30. C. D'Souza-Schorey, R. L. Boshans, M. McDonough, P. D. Stahl, L. Van Aelst, *EMBO J.* **16**, 5445 (1997).
31. H. Van Valkenburgh, J. F. Shern, J. D. Sharer, X. Zhu, R. A. Kahn, *J. Biol. Chem.* **276**, 22826 (2001).
32. B. J. Peter, unpublished data.
33. B. J. Peter and P. J. G. Butler, analytical ultracentrifugation data (see fig. S1).
34. PICK1 has an N-terminal PDZ domain and a C-terminal BAR domain. The PDZ domain binds and clusters metabotropic glutamate receptors (*49*) and AMPA receptors (*50*) and is important in their localization. We could not get good expression of this protein, but we suggest that the BAR domain (while dimerizing the proteins and thus aggregating the receptors) will localize these channels to areas of preferred membrane curvature. ICA69 (islet cell autoantigen of 69 kD) is a diabetes-associated protein related to arfaptin. Although its exact function is unknown, ICA69 is localized to the TGN and is involved in secretion (*51*, *52*).
35. T. R. Jackson, B. G. Kearns, A. B. Theibert, *Trends Biochem. Sci.* **25**, 489 (2000).
36. P. A. Randazzo *et al.*, *Proc. Natl. Acad. Sci. U.S.A.* **97**, 4011 (2000).
37. Z. Nie *et al.*, *J. Biol. Chem.* **277**, 48965 (2002).
38. Both centaurin and oligophrenin bound efficiently to liposomes but tubulated poorly compared with amphiphysin and arfaptin. Thus, higher protein concentrations, 2 to 5 times those of amphiphysin and arfaptin (30 μM in the case of oligophrenin), were required to see tubulation. We did not observe in vivo tubulation with the BAR + PH domain of oligophrenin, but this could be caused by the N-terminal Myc tag.
39. F. Fauchereau *et al.*, *Mol. Cell. Neurosci.* **23**, 574 (2003).
40. P. Billuart *et al.*, *Pathol. Biol.* **46**, 678 (1998).
41. J. D. Hildebrand, J. M. Taylor, J. T. Parsons, *Mol. Cell. Biol.* **16**, 3169 (1996).
42. X. R. Ren *et al.*, *J. Cell Biol.* **152**, 971 (2001).
43. Dab2 PTB domain binds liposomes containing PtdIns(4,5)P_2 but does not tubulate them.
44. M. G. Ford *et al.*, *Nature* **419**, 361 (2002).
45. Reducing the binding to liposomes was not sufficient to cause BAR proteins to be curvature-sensitive in this assay. Although the mut1 and F9E mutants of amphiphysin1 bound liposomes more weakly than the wild-type (Fig. 2D), neither showed a curvature preference. Furthermore, the centaurinβ2 BAR and BAR + PH proteins had different binding affinities, yet they had similar curvature sensitivity (Figs. 4B and 5B).
46. C. Reinhard, M. Schweikert, F. T. Wieland, W. Nickel, *Proc. Natl. Acad. Sci. U.S.A.* **100**, 8253 (2003).
47. X. Bi, R. A. Corpina, J. Goldberg, *Nature* **419**, 271 (2002).
48. The amphiphysin BAR domain has a general positive charge over the concave surface and, in our experiments, preferred PtdIns(4,5)P_2 over PtdIns(4)P or PtdIns(3)P. Other BAR domains shared this preference for more negatively charged lipids. Full-length arfaptin preferred PtdIns(4)P, but the lipid specificity seemed to be determined by the N-terminus, which contains a lipid-binding domain (Fig. 3B and B. J. Peter, unpublished data).
49. H. Boudin *et al.*, *Neuron* **28**, 485 (2000).
50. J. Xia, X. Zhang, J. Staudinger, R. L. Huganir, *Neuron* **22**, 179 (1999).
51. M. Pilon, X. R. Peng, A. M. Spence, R. H. Plasterk, H. M. Dosch, *Mol. Biol. Cell* **11**, 3277 (2000).
52. F. Spitzenberger *et al.*, *J. Biol. Chem.* **278**, 26166 (2003).
53. Single-letter abbreviations for the amino acid residues are as follows: A, Ala; C, Cys; D, Asp; E, Glu; F, Phe; G, Gly; H, His; I, Ile; K, Lys; L, Leu; M, Met; N, Asn; P, Pro; Q, Gln; R, Arg; S, Ser; T, Thr; V, Val; W, Trp; and Y, Tyr.
54. M. A. Salazar *et al.*, *J. Biol. Chem.* **278**, 49031 (2003).
55. www.ncbi.nlm.nih.gov/Structure/cdd/cddfind.cgi
56. L. D. Mayer, M. J. Hope, P. R. Cullis, *Biochim. Biophys. Acta* **858**, 161 (1986).

57. We thank the Kazusa DNA Research Institute, the I.M.A.G.E. consortium, S. Gamblin, and M. Lazdunski for sharing plasmids; A. Thompson for help at the ESRF; and G. Praefcke for purified Dab2. I.G.M. was supported by an MRC postdoctoral fellowship, and B.J.P. was supported by an EMBO long-term postdoctoral fellowship.

Supporting Online Material

www.sciencemag.org/cgi/content/full/1092586/DC1
Materials and Methods
Figs. S1 to S6
Table S1
References and Notes

15 October 2003; accepted 18 November 2003
Published online 27 November 2003;
10.1126/science.1092586
Include this information when citing this paper.

REPORTS

Detection of a Red Supergiant Progenitor Star of a Type II–Plateau Supernova

Stephen J. Smartt,[1]* Justyn R. Maund,[1] Margaret A. Hendry,[1] Christopher A. Tout,[1] Gerard F. Gilmore,[1] Seppo Mattila,[2] Chris R. Benn[3]

We present the discovery of a red supergiant star that exploded as supernova 2003gd in the nearby spiral galaxy M74. The Hubble Space Telescope (HST) and the Gemini Telescope imaged this galaxy 6 to 9 months before the supernova explosion, and subsequent HST images confirm the positional coincidence of the supernova with a single resolved star that is a red supergiant of 8^{+4}_{-2} solar masses. This confirms both stellar evolution models and supernova theories predicting that cool red supergiants are the immediate progenitor stars of type II–plateau supernovae.

Supernova (SN) 2003gd was discovered on 12.82 June universal time in the nearby spiral galaxy M74 (*1*). It was rapidly shown to be a type II–plateau (II-P) SN that was discovered about 87 days after explosion (*2*–*5*). The progenitors of type II-P SNe have long been thought to be red supergiant stars with initial masses greater than 8 to 10 solar masses ($M_\odot$) that have retained their hydrogen envelopes before core collapse. This model accounts for the 2- to 3-month-long plateau phases seen in the lightcurves of SNe II-P, the existence of hydrogen P-Cygni profiles (which are indicative of an optically thick expanding atmosphere) in the early time spectra, and the estimated physical parameters of the expanding photosphere such as velocity, temperature, and density (*6*–*8*). Stellar evolutionary calculations are consistent with this picture, in which stars with initial masses in the range

[1]Institute of Astronomy, University of Cambridge, Madingley Road, Cambridge CB3 0HA, UK. [2]Stockholm Observatory, AlbaNova University Center, SE-106 91 Stockholm, Sweden. [3]Isaac Newton Group of Telescopes, Apartado 321, Santa Cruz de La Palma E-38700, Spain.

*To whom correspondence should be addressed. E-mail: sjs@ast.cam.ac.uk